Phase transition and thermodynamic properties of $BiFeO_3$ from first-principles calculations*

Li Qiang(李 强), Huang Duo-Hui(黄多辉), Cao Qi-Long(曹启龙), and Wang Fan-Hou(王藩侯)†

Key Laboratory of Computational Physics of Sichuan Province, Yibin University, Yibin 644000, *China*

(Received 4 July 2012; revised manuscript received 15 August 2012)

The first-principles projector-augmented wave method employing the quasi-harmonic Debye model, is applied to investigate the thermodynamic properties and the phase transition between the trigonal *R*3*c* structure and the orthorhombic *Pnma* structure. It is found that at ambient temperature, the phase transition from the trigonal *R*3*c* phase to the orthorhombic *Pnma* phase is a first-order antiferromagnetic–nonmagnetic and insulator–metal transition, and occurs at 10.56 GPa, which is in good agreement with experimental data. With increasing temperature, the transition pressure decreases almost linearly. Moreover, the thermodynamic properties including Grüneisen parameter, heat capacity, entropy, and the dependences of thermal expansion coefficient on temperature and pressure are also obtained.

Keywords: first-principles calculation, $BiFeO_3$, thermodynamic property, phase transition

PACS: 71.15.Mb, 64.70.K−, 65.40.–b **DOI:** 10.1088/1674-1056/22/3/037101

1. Introduction

Bismuth ferrite ($BiFeO_3$) has attracted increasingly attention in recent years due to both ferroelectric and magnetic orders at room temperature,[1–4] and the potential technological applications in novel magnetoelectric devices and theoretical and experimental research, especially in thin-film cases.[5] As a room-temperature multiferroic material, $BiFeO_3$ is a trigonal ferroelectric perovskite with space group *R*3*c*, possesses high spontaneous electric polarization below the ferroelectric Curie temperature of 1100 K, and shows a G-type antiferromagnetic order below the Néel temperature of 643 K.[6] Although there are abundant studies on bulk $BiFeO_3$, it still has some controversy about its phase transition. A great deal of experimental effort has been devoted to settle this issue. Gavriliuk *et al.*[7] investigated the pressure-induced spin crossover in $BiFeO_3$ and the insulator–metal transition at the same pressures by using synchrotron X-ray diffraction, nuclear forward scattering, X-ray emission, the optical absorption, and dc resistivity measurements. They claimed that the reversible insulator–metal Mott transition was observed at pressures higher than 55 GPa. According to compression experiments[8] performed using diamond anvil cells, structural transformations of $BiFeO_3$ were found in the range of 40–55 GPa. The studies on the magnetic behavior of $BiFeO_3$,[9] using the methods of nuclear forward scattering (NFS) of synchrotron radiation, suggested that the field H^{Fe} abruptly dropped to zero in the pressure interval $47 < P < 61.4$ GPa, testifying a transition from antiferromagnetic to a nonmagnetic state. Recent experiments[10,11] have proposed that the magnetic and electric phase transitions occur above 45 GPa in $BiFeO_3$, but phase transitions below 45 GPa are not observed. In the theoretical research of the phase transition of $BiFeO_3$, González–Vázquez and Íñiguez[12] performed a first-principles study and predicted that the phase transition in $BiFeO_3$ occurs at pressure of about 40 GPa. However, we also notice that some researchers drew different conclusions. For instance, Haumont *et al.*[13] reported that with increasing pressure, the cation displacements of $BiFeO_3$ are reduced and finally suppressed at around 10 GPa, leading to the non-polar *Pnma* structure by using diffraction and far-infrared spectroscopy from synchrotron sources. Moreover, Ravindran *et al.*[14] have predicted a single pressure-induced structural transition from the initial trigonal *R*3*c* structure to an orthorhombic *Pnma* ($GdFeO_3$-type) structure at around 13 GPa based on the *ab initio* calculations. Despite the experimental and theoretical effort, a consensus about the pressure-induced phase transition for $BiFeO_3$ has not yet been reached. Thus, the aim of our study is to verify the occurrence of the pressure-induced phase transition from the initial trigonal structure with space group *R*3*c* to an orthorhombic structure with space group *Pnma* below 20 GPa, and to evaluate the thermodynamic properties of both phases. The quasi-harmonic Debye model, which well predicts various properties,[15–20] such as thermodynamic properties and the phase transition, has been selected for the purpose. To our best knowledge, it is the first time that the transition pressure from trigonal *R*3*c*-$BiFeO_3$ to orthorhombic *Pnma*-$BiFeO_3$ in the temperature range of 0–1200 K has been obtained theoretically.

The paper is organized as follows. Theoretical methods are shown in Section 2. In Section 3, the calculation results are given and discussed. Finally, the conclusions of this work

*Project supported by the Foundation of Key Laboratory of National Defense Science and Technology for Shock Wave and Detonation Physics, China and the Science and Research Foundation of Educational Committee of Sichuan Province, China (Grant No. 09ZC048).

†Corresponding author. E-mail: wslypq@126.com

© 2013 Chinese Physical Society and IOP Publishing Ltd

are presented.

2. Theoretical methods

The first-principles calculations are performed based on the Vienna *ab initio* simulation package (VASP).[21] The electron–ion interactions are treated within the projector-augmented wave.[22] The exchange correlation potential is described by the generalized gradient approximation (GGA) of PBE.[23] For the Brillouin zone sampling, 4×4×4 and 4×4×2 Monkhorst–Pack meshes[24] are used for the trigonal *R*3*c*-$BiFeO_3$ and the orthorhombic *Pnma*-$BiFeO_3$, respectively. According to the test results, the electronic wavefunctions are expanded in a plane-wave basis set with an energy cutoff of 293.2 eV. The allowed error in total energy is smaller than 10^{-4} eV per atom between two electronic self-consistent steps. The change in the total free energy is smaller than -10^{-3} eV per atom between two ionic steps. Thermodynamic calculations are performed by Gibbs2.[25]

Within the framework of the quasi-harmonic Debye model, the non-equilibrium Gibbs free energy $G(V,P,T)$ is usually given by[25]

$$G(V,P,T) = E(V) + PV + F_{\rm vib}(\Theta(V),T), \tag{1}$$

where $E(V)$ represents the static energy without zero-point vibrational energy from the first-principles total energy calculations fitted by an equation of state at 0 K and volume V, PV corresponds to the constant hydrostatic pressure condition, P is the pressure, V is the volume, and $\Theta(V)$ is the Debye temperature. Vibrational free energy can be calculated by the empirical Debye model as follows:[25]

$$F_{\rm vib}(\Theta,T) = nkT\left[\frac{9}{8}\frac{\Theta}{T} + 3\ln(1-{\rm e}^{-\Theta/T}) - D(\Theta/T)\right], \tag{2}$$

where n is the number of atoms per formula cell, K is the Boltzmann's constant, T is the temperature in Kelvin, and $D(\Theta/T)$ is the Debye integral. Debye temperature can be written as[25]

$$\Theta = \frac{\hbar}{K}[6\pi^2 V^{1/2} n]^{1/3} f(\sigma)\sqrt{\frac{B_{\rm s}}{M}}, \tag{3}$$

$$B_{\rm s} \approx B_{\rm static}(V) \approx B_{\rm static}(V_{\rm opt}) = V\left(\frac{{\rm d}^2 E(V)}{{\rm d}V^2}\right), \tag{4}$$

where M is the molecular mass per unit cell; $B_{\rm s}$ is the adiabatic bulk modulus,[26] which is approximated by the static compressibility; σ is Poisson's ratio. The form of $f(\sigma)$ is given as follows:[27]

$$f(\sigma) = \left\{3\left[2\left(\frac{2}{3}\frac{1+\sigma}{1-2\sigma}\right)^{3/2} + \left(\frac{1}{3}\frac{1+\sigma}{1-\sigma}\right)^{3/2}\right]^{-1}\right\}^{1/3}. \tag{5}$$

The non-equilibrium Gibbs function $G^*(V;P,T)$ can be minimized with respect to volume V[25]

$$\left(\frac{\partial G^*(V;P,T)}{\partial V}\right)_{P,T} = 0. \tag{6}$$

The heat capacity $C_{\rm V}$, the thermal expansion coefficient α, and the Grüneisen constant γ are expressed as[25]

$$C_{\rm V} = 3nk\left[4D(\Theta/T) - \frac{3\Theta/T}{{\rm e}^{\Theta/T}-1}\right], \tag{7}$$

$$\alpha = \gamma C_{\rm V}/(B_{\rm T}V), \tag{8}$$

$$\gamma = \frac{{\rm d}\ln\theta(V)}{{\rm d}\ln V}, \tag{9}$$

where $B_{\rm T}$ is the isothermal thermal bulk modulus. The calculated static energies by using first-principles method with respect to the volume are fitted to the third-order Birch–Murnaghan equation of state[26]

$$\begin{aligned} E(V) &= E_0 + \frac{9V_0B_0}{16}\{[(V_0/V)^{2/3}-1]^3B_0' \\ &\quad + [(V_0/V)^{2/3}-1]^2[6-4(V_0/V)^{2/3}]\}. \end{aligned} \tag{10}$$

The relationship[26] between the pressure P and the volume V can be obtained by

$$\begin{aligned} P(V) &= \frac{3B_0}{2}[(V_0/V)^{7/3} - (V_0/V)^{5/3}] \\ &\quad \times \left\{1 + \frac{3}{4}(B_0'-4)[(V_0/V)^{2/3}-1]\right\}. \end{aligned} \tag{11}$$

Through the quasi-harmonic Debye model, the thermodynamic parameters of $BiFeO_3$ at any pressures and temperatures from the calculated $E(V)$ data at $T = 0$ K and $P = 0$ GPa can be obtained.

3. Results and discussion

3.1. Equation of state

The equation of state for crystalline materials is of importance in many applications. It can provide a convenient measure of the expansion coefficient and the compressibility coefficient. A series of *ab initio* simulations for the *R*3*c*-$BiFeO_3$ and the *Pnma*-$BiFeO_3$ have been performed to obtain E–V data, which is shown in Fig. 1. It can be seen that the *R*3*c*-$BiFeO_3$ is more stable than the *Pnma*-$BiFeO_3$ at zero temperature and zero pressure.

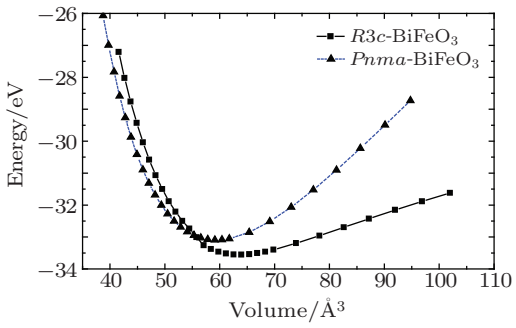


Fig. 1. Fitted total energy per formula unit as a function of volume for the *R*3*c*-$BiFeO_3$ and the *Pnma*-$BiFeO_3$ from the third-order Birch–Murnaghan equation of state.

The calculated lattice parameter a_0, bulk modulus B_0, and its first derivate B_0' for both phases by using the third-order Birch–Murnaghan equation of state are listed in Table 1 to compare with experimental and other calculated data. It is found that our calculated results are in agreement with the experimental data[7,13,31,32] and other theoretical results.[14,27–30]

Table 1. Lattice constants, bulk modulus, and its pressure derivation of the $R3c$-$BiFeO_3$ and the $Pnma$-$BiFeO_3$ at 0 GPa and 0 K.

	$R3c$-$BiFeO_3$				$Pnma$-$BiFeO_3$		
	This work	Theor.	Exp.		This work	Theor.	Exp.
a/Å	5.613	5.459[a]	5.634[f]	a/Å	5.502	5.585[c]	5.495[e]
		5.500[b]	5.630[g]				
α/(°)	59.687	60.360[a]	59.348[f]	b/Å	7.782	7.660[c]	7.650[e]
		60.180[b]	59.343[g]				
V/Å^3	124.1	116.0[a]	124.3[f]	c/Å	5.129	5.350[c]	5.327[e]
		115.0[b]	124.6[g]				
B_0	137.7	130.9[c]	75.5±15.5[h]	B_0	149.3	138.8[c]	–
		130.0[d]	116.0[e]				
B_0'	3.75	–	3.70[e]	B_0'	4.20	–	–

[a] Ref. [27], [28], [b] Ref. [29], [30], [c] Ref. [14], [d] Ref. [12], [e] Ref. [13], [f] Ref. [31], [g] Ref. [32], [h] Ref. [7].

When the temperature is zero, the Gibbs free energy equals the enthalpy ($H = U + PV$). It is easy to obtain the enthalpy of the $R3c$-$BiFeO_3$ and the $Pnma$-$BiFeO_3$ by Eqs. (11) and (12). The calculated H–P data are shown in Fig. 2. It is found that the transition pressure from the $R3c$-$BiFeO_3$ to the $Pnma$-$BiFeO_3$ is 12.05 GPa, which is in agreement with the predicted value of 13 GPa[14] from recent *ab initio* calculations. At 0 K, the $R3c$-$BiFeO_3$ is more stable than the $Pnma$-$BiFeO_3$ below 12.05 GPa, but the $Pnma$-$BiFeO_3$ is more stable than the $R3c$-$BiFeO_3$ above 12.05 GPa.

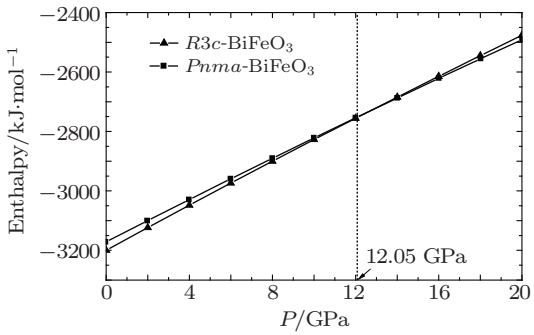


Fig. 2. Enthalpy with pressure for $BiFeO_3$.

3.2. Magnetic ground state

In order to determine the stable magnetic ground state of the $R3c$-$BiFeO_3$ and the $Pnma$-$BiFeO_3$, we take the following steps. Firstly, according to anti-parallel and parallel spins for Fe atoms, respectively, the appropriate cell parameters of both phases have been obtained after optimizing the lattice constants and internal atom coordinates based on the principle of energy minimization. Secondly, the total energy calculations for both phases were performed in antiferromagnetic (AFM) and ferromagnetic (FM) states with the first-principles approach, respectively. The calculated results for both phases in AFM and FM states are listed in Table 2. As seen in Table 2, the $R3c$-$BiFeO_3$ shows an AFM ground state because of the energy difference ΔE (−0.615 eV) between the AFM and FM states. The energy difference ΔE for the $Pnma$-$BiFeO_3$ between AFM and FM states is nearly equal to 0 eV, which indicates that the phase is nonmagnetic.

Table 2. Ground states of the $R3c$-$BiFeO_3$ and the $Pnma$-$BiFeO_3$ are shown, where FM, NM, and AFM represent ferromagnetic, nonmagnetic, and antiferromagnetic states, respectively. The energy difference (ΔE) between the AFM and FM states and the binding energy (E_b) per atom are presented.

Phase	Ground state	E_b/meV	ΔE/eV	E_{AFM}/eV	E_{FM}/eV
$R3c$-$BiFeO_3$	AFM	237.966	–0.615	–67.095	–66.480
$Pnma$-$BiFeO_3$	NM	229.566	0.008	–132.510	–132.512

Because the binding energy generally describes the relative phase stability, it is necessary to calculate the binding energy of the $R3c$-$BiFeO_3$ and the $Pnma$-$BiFeO_3$. The binding energy per atom for both phases is given by

$$E_b = \Big(\sum n_i E(\mathrm{Fe}) + \sum n_j E(\mathrm{Bi}) + \sum n_z E(\mathrm{O}) - E(\mathrm{perfect})\Big)/(n_i + n_j + n_z), \quad (12)$$

where $E(\mathrm{perfect})$ is the total energy of the $R3c$-$BiFeO_3$ or $Pnma$-$BiFeO_3$, n_i, n_j, and n_z are the number of Fe, Bi, and O atoms in the crystal structure, and E (Fe), E (Bi), and E (O) are the average energy of an atom in the bulk or molecule, respectively. It can be seen from Table 2 that the binding energy of $R3c$-$BiFeO_3$ is larger than that of $Pnma$-$BiFeO_3$, which indicates the $R3c$-$BiFeO_3$ is more stable than the $Pnma$-$BiFeO_3$ at zero temperature and zero pressure, which is consistent with the previous analysis of the equation of state.

3.3. Electronic structure

In the following, the electronic structures of $BiFeO_3$ at its equilibrium structure are calculated. The predicted total and partial density of states for $R3c$-$BiFeO_3$ are shown in Fig. 3. The Fermi level is set to zero. From Fig. 3, it can be seen that both the major spin total density of states (TDOS) are equal to the minor spin one, which is due to the AFM nature of $R3c$-$BiFeO_3$. Both Bi and O partial density of states (PDOS) are also equal in the spin-up and spin-down states. The Fe PDOS is quite different for the two spin states (spin up and spin down, Fe1 and Fe2), which means that the $R3c$-$BiFeO_3$ is antiferromagnetic. The valence band (VB) in the range from −19.7 to −17.3 eV is mainly occupied by O 2s states. The Bi 6s states are located at around −10 eV. The valence band in the range from −6.7 to 0 eV consists of O 2p states mixed with Fe 3d and Bi 6p states. Above the Fermi level, the conduction band (CB) is dominated by Fe 3d states in the range of 0.5–3.6 eV and Bi 6p states in the region of 3.6–5.5 eV. These states are strongly mixed with O 2p states. In addition, the calculated magnetic moment at the Fe site is 3.69 μ_B, which is in good agreement with the value of 3.75 μ_B[33] measured from low-temperature neutron-diffraction measurements. Since the Fe electrons mix with the neighboring O ions, the calculated magnetic moment at the Fe sites are not integer values, and the O ions have a slight magnetic moment of 0.07 μ_B. The $R3c$-$BiFeO_3$ shows a gap of about 0.8 eV, which indicates that the $BiFeO_3$ phase with space group $R3c$ is a semiconductor and considered to be determined by the charge-transfer transitions from the occupied O 2p to unoccupied Fe 3d states, as suggested by experiments[34] and *ab initio* calculations.[35]

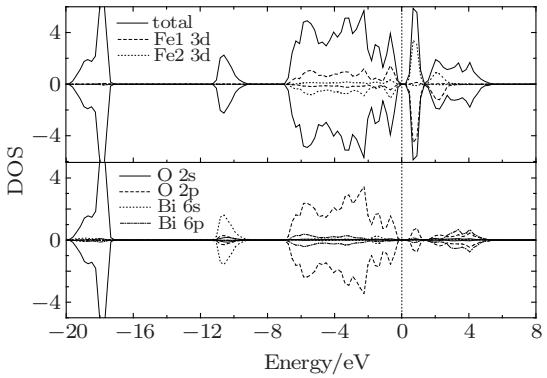


Fig. 3. Calculated total and partial density of states for $BiFeO_3$ in AFM $R3c$ phase.

The calculated total and partial density of states for the $Pnma$-$BiFeO_3$ structure are also shown in Fig. 4. It is found that in the valence band, the TDOS in the range from −20 to −18 eV are mainly occupied by O 2s states. The Bi 6s states are located at around -11 eV below the Fermi level. In the range from −7.3 to −1 eV, the O 2p states mingle obviously with Fe 3d and Bi 6p states. Above the Fermi level, the conduction band (CB) is dominated by Fe 3d states in the range of 0–4 eV, and Bi 6p states in the region from 2 to 4 eV. These states strongly mix with O 2p states. It is noted that the states in the range from −1.1 to 0.5 eV mainly originate from Fe 3d states, which means that the $Pnma$-$BiFeO_3$ is metallic.

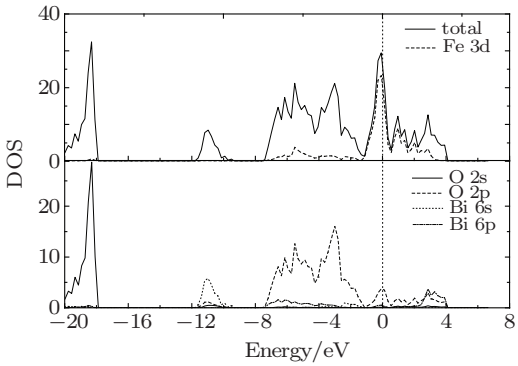


Fig. 4. Calculated total and partial density of states for $BiFeO_3$ in NM $Pnma$ phase.

3.4. Phase transition

To clearly clarify the phase transition at any pressure and any temperature, more investigations are preformed by using a quasi-harmonic Debye model. According to thermodynamics knowledge, at the transition point, the Gibbs free energies of two phases are equal. Therefore, the phase transition pressure and temperature from the $R3c$-$BiFeO_3$ to the $Pnma$-$BiFeO_3$ can be evaluated from the usual condition of equal Gibbs free energies, i.e., the pressures at which the Gibbs free energies of both phases are the same.[36]

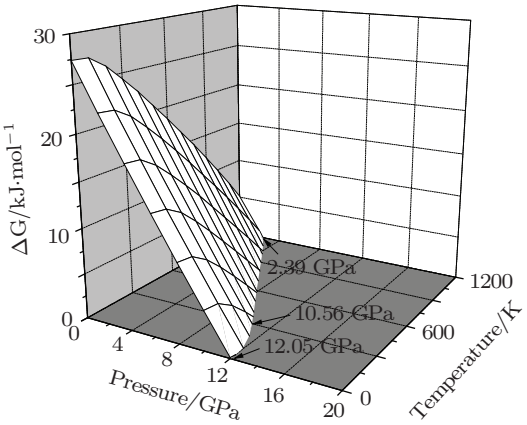


Fig. 5. Gibbs free energy as a function of pressure for $BiFeO_3$.

The Gibbs free energies are calculated at different temperatures and pressures. The difference in Gibbs free energy between the $R3c$-$BiFeO_3$ and the $Pnma$-$BiFeO_3$ $\Delta G = G_{Pnma} - G_{R3c}$ is shown in Fig. 5 for different temperatures and pressures. From Fig. 5, it is found that when $P = 12.05$ GPa at 0 K, $\Delta G = 0$. This means that at zero temperature the transition pressure is 12.05 GPa, which is in agreement with the theoretical result[14] and the above analysis of binding energy and enthalpy of both phases, and the $R3c$-$BiFeO_3$ is more stable

than the *Pnma*-$BiFeO_3$ when the pressure is below 12.05 GPa. At 298.15 K, the pressure is 10.56 GPa, and $\Delta G = 0$. This indicates that at room temperature, the phase transition from the *R*3*c*-$BiFeO_3$ to the *Pnma*-$BiFeO_3$ occurs at 10.56 GPa, which is in good agreement with the experimental value of 10 GPa[13] by using diffraction and far-infrared spectroscopy from synchrotron sources, and the *R*3*c*-$BiFeO_3$ is more stable than the *Pnma*-$BiFeO_3$ when the pressure is below 10.56 GPa. The phase transition will not occur, even at 1200 K when the pressure is below 2.39 GPa. When the temperature is fixed, ΔG increases with decreasing pressure. This means that the *R*3*c*-$BiFeO_3$ becomes increasingly stable compared with the *Pnma*-$BiFeO_3$. At zero pressure, ΔG is positive in the range of 0–1200 K, which implies that the *R*3*c*-$BiFeO_3$ phase is more stable than the *Pnma*-$BiFeO_3$ phase. It can be observed that the transition pressure decreases with increasing temperature above room temperature. By fitting these data to third-order polynomials in temperature, the following relationship can be obtained

$$P_{\mathrm{T}} = 12.0511 - 0.00285T - 8.9025 \times 10^{-6}T^2 + 3.89175 \times 10^{-9}T^3. \quad (13)$$

Therefore, the phase transition from the *R*3*c*-$BiFeO_3$ to the *Pnma*-$BiFeO_3$ is a first-order antiferromagnetic–nonmagnetic and insulator–metal transition due to the disappearance of antiferromagnetic state, the appearance of nonmagnetic state, the change in the electronic structures, and the huge structural difference between the *R*3*c*-$BiFeO_3$ and the *Pnma*-$BiFeO_3$.

3.5. Thermodynamic properties

Thermodynamic properties play an important role in understanding the thermal response of materials. Since $BiFeO_3$ is a potential material for magnetoelectric devices, it is necessary to investigate the thermodynamic properties at different temperatures and pressures. Thus, we can determine the environment which $BiFeO_3$ can work in. Through the quasi-harmonic Debye model, the Grüneisen parameter γ, the heat capacities C_{V} and C_{P}, vibrational entropy S_{vib}, and thermal expansion coefficient α of $BiFeO_3$ at different temperatures and different pressures have been calculated.

Grüneisen constant γ describes the alteration in vibration frequency of a crystal lattice, and it has been widely used to characterize and extrapolate the thermodynamic behavior of a material at high pressures and temperatures. The Grüneisen parameter γ at different temperatures (0–1200 K) and different pressures (0–20 GPa) is obtained, which are listed in Table 3. It is noted that the Grüneisen constant γ of both phases decreases with the increase in pressure at a given temperature, and increases with the increase in temperature at a given pressure.

Table 3. Grüneisen constant γ of the *R*3*c*-$BiFeO_3$ and the *Pnma*-$BiFeO_3$ at different temperatures and pressures.

Phase	*P*/GPa	300 K	600 K	900 K	1200 K
*R*3*c*-$BiFeO_3$	0	1.740	1.766	1.793	1.820
	5	1.675	1.698	1.722	1.747
	10	1.623	1.640	1.661	1.684
	20	1.543	1.553	1.564	1.578
Pnma-$BiFeO_3$	0	1.970	2.004	2.046	2.096
	5	1.900	1.925	1.955	1.990
	10	1.847	1.866	1.888	1.914
	20	1.769	1.782	1.796	1.811

The heat capacity predicted for the *R*3*c*-$BiFeO_3$ and the *Pnma*-$BiFeO_3$ at constant pressure and constant volume by the quasi-harmonic Debye model are shown in Figs. 6 and 7, respectively. From Fig. 6, it is can be seen that the heat capacity C_{P} of the *R*3*c*-$BiFeO_3$ and the *Pnma*-$BiFeO_3$ at zero pressure increases sharply below 300 K, and then the increasing trend becomes slower at high temperature. The predicted heat capacity C_{P} for the *R*3*c*-$BiFeO_3$ at 0 GPa is in agreement with the experimental results[37–40] and the theoretical data.[41] It is noted that the heat capacity of *R*3*c*-$BiFeO_3$ is lower than that of *Pnma*-$BiFeO_3$ in the whole temperature range of interest. From Fig. 7, the increasing trend of C_{V} at low temperature is similar to C_{P}, but C_{V} in both phases approaches the Dulong–Petit limit of $3nN_{\mathrm{A}}k_{\mathrm{B}}$, which is common to all solids at high temperatures.

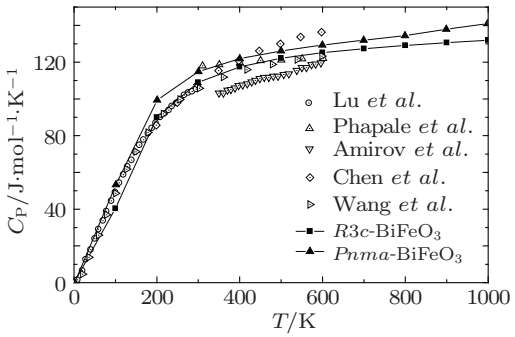


Fig. 6. Heat capacity C_{P} as a function of temperature for the *R*3*c*-$BiFeO_3$ and the *Pnma*-$BiFeO_3$ at zero pressure. Experimental results[37–40] and other theoretical data[41] for the *R*3*c*-$BiFeO_3$ are shown for comparison.

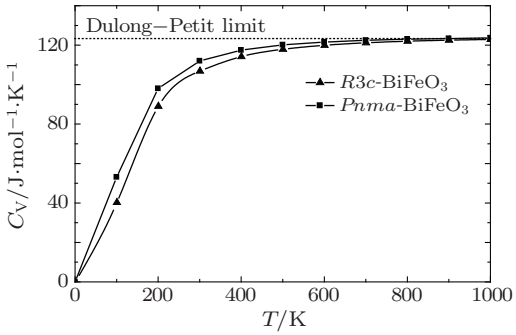


Fig. 7. Heat capacity C_{V} as a function of temperature for the *R*3*c*-$BiFeO_3$ and the *Pnma*-$BiFeO_3$ at zero pressure.

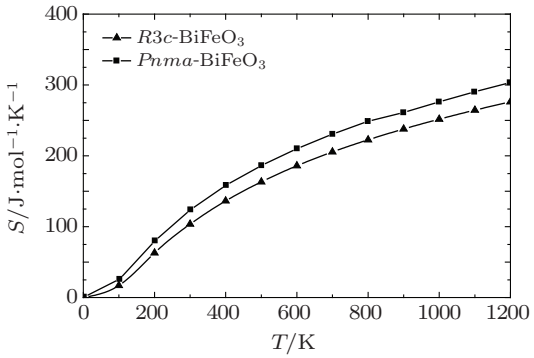


Fig. 8. Entropy for $BiFeO_3$ as a function of temperature at zero pressure.

Based on the quasi-harmonic Debye model, vibrational entropy S_{vib} as a function of temperature is calculated and shown in Fig. 8. It can be observed that the entropy increases monotonically with temperature. The vibrational entropy of $R3c$-$BiFeO_3$ is lower than that of *Pnma*-$BiFeO_3$ at high temperatures due to different bond strengths.

$BiFeO_3$ is a potential semiconductor and photocatalytic material, and hence it is necessary to investigate the thermal expansion coefficient of its thin film. It is noted that there are certain difficulties associated with the measurement of thermal expansion coefficient at high temperatures, which lead to considerable uncertainties in the experimental values,[42] so the theoretical investigate is performed by using the quasi-harmonic Debye model. The calculated pressure and temperature dependences of the thermal expansion coefficient α of $R3c$-$BiFeO_3$ and *Pnma*-$BiFeO_3$ are plotted in Fig. 9.

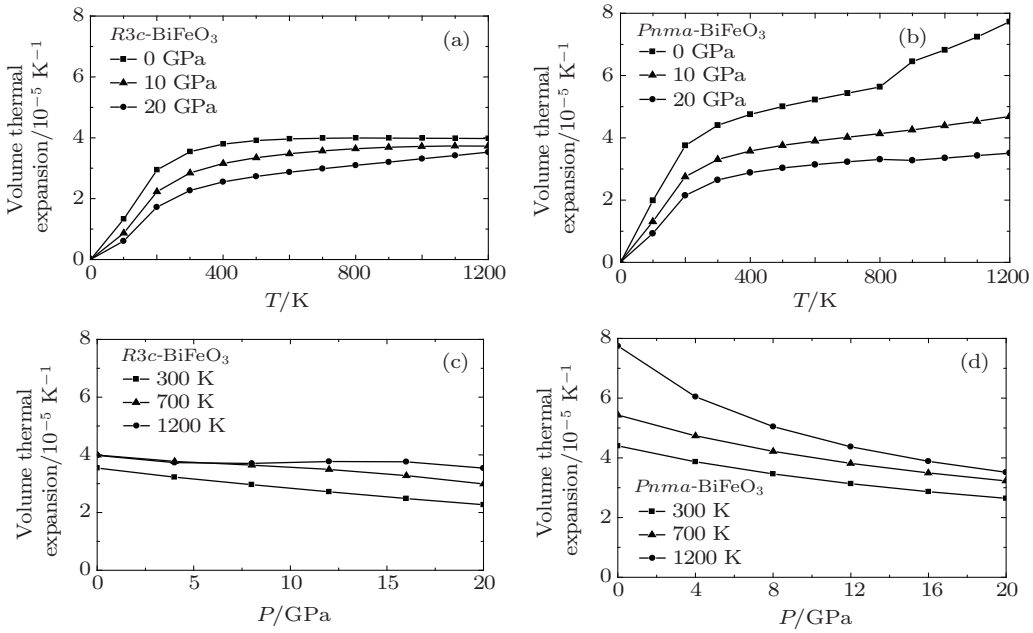


Fig. 9. Variations of thermal expansion coefficient with temperature and pressure for (a, c) $R3c$-$BiFeO_3$ and (b, d) *Pnma*-$BiFeO_3$.

From Figs. 9(a) and 9(b), it can be seen that as temperature increases, the thermal expansion coefficient of both phases increases rapidly below 300 K, and gradually turns into a linear increase at high temperatures. As shown in Figs. 9(c) and 9(d), the thermal expansion coefficient of both phases decreases rapidly with increasing pressure, and almost exponentially except that of $R3c$-$BiFeO_3$ at 300 K because of the occurrence of phase transition at around 10.56 GPa. It is found that the *Pnma*-$BiFeO_3$ is more sensitive to temperature compared with the $R3c$-$BiFeO_3$. At the same temperature and pressure, the $R3c$-$BiFeO_3$ has a lower thermal expansion, which is more favorable for thin film of $BiFeO_3$.

4. Conclusions

The transition phase of $BiFeO_3$ from the trigonal $R3c$ structure to the orthorhombic *Pnma* structure has been investigated by using the first-principles projector-augmented wave method, together with quasi-harmonic Debye model. It is found that the phase transition from the trigonal $R3c$ phase to the orthorhombic *Pnma* phase is a first-order antiferromagnetic–nonmagnetic and insulator–metal transition according to the usual condition of equal Gibbs free energies, and occurs at 10.56 GPa, which is in good agreement with the experimental data. The transition pressure decreases almost linearly with temperature. Through the quasi-harmonic Debye model, the heat capacity C_V and C_P, vibrational entropy S_{vib}, thermal expansion α, and the Grüneisen parameter γ of both phases at different temperatures and pressures are obtained, and compared with available experimental data.

References

[1] Fischer P, Polomska M, Sosnowska I and Szymanski M 1980 *J. Phys. C* **13** 1931

[2] Wang J, Neaton J B, Zheng H, Nagarajan V, Ogale S B, Liu B, Viehland D, Vaithyanathan V, Schlom D G, Waghmare U V, Spaldin N A, Rabe K M, Wuttig M and Ramesh R 2003 *Science* **299** 1719

[3] Kornev I A, Lisenkov S, Haumont R, Dkhil B and Bellaiche L 2007 *Phys. Rev. Lett.* **99** 227602

[4] Ihlefeld J F, Podraza N J, Liu Z K, Rai R C, Xu X, Heeg T, Chen Y B, Li J, Collins R W, Musfeldt J L, Pan X Q, Schubert J, Ramesh R and Schlom1 D G 2008 *Appl. Phys. Lett.* **92** 142908

[5] Ramesh R and Spaldin N A 2007 *Nat. Mater.* **6** 21

[6] Venevtsev Y N, Gagulin V V and Viscov A S 1995 *Ferroelectrics* **167** 289

[7] Gavriliuk A G, Struzhkin V V, Lyubutin I S, Ovchinnikov S G, Hu M Y and Chow P 2008 *Phys. Rev. B* **77** 155112

[8] Gavriliuk A G, Struzhkin V V, Lyubutin I S, Trojan A, Hu M Y and Chow P 2006 *MRS Proceedings* **987** 0987-PP05-02

[9] Gavriliuk A G, Struzhkin V V, Lyubutin I S, Hu M Y and Mao H K 2005 *JETP Lett.* **82** 224

[10] Gavriliuk A G, Lyubutin I S and Struzhkin V V 2007 *JETP Lett.* **86** 532

[11] Scott J F, Palai R, Kumar A, Singh M K, Murari N M, Karan N K and Katiyar R S 2008 *J. Am. Cer. Soc.* **91** 1762

[12] González-Vázquez O E and Íñiguez J 2009 *Phys. Rev. B* **79** 064102

[13] Haumont R, Bouvier P, Pashkin A, Rabia K, Frank S, Dkhil B, Crichton W A, Kuntscher C A and Kreisel J 2009 *Phys. Rev. B* **79** 184110

[14] Ravindran P, Vidya R, Kjekshus A, Fjellvåg H and Eriksson O 2006 *Phys. Rev. B* **74** 224412

[15] Liu L, Wei J J, An X Y, Wang X M, Liu H N and Wu W D 2011 *Chin. Phys. B* **20** 106201

[16] Yu B H and Chen D 2011 *Chin. Phys. B* **20** 030508

[17] Yu J X, Fu M, Ji G F and Chen X R 2009 *Chin. Phys. B* **18** 269

[18] Zhang W, Cheng Y, Zhu J and Chen X R 2009 *Chin. Phys. B* **18** 1207

[19] Wu J H, Zhao X L, Song Y L and Wu G D 2011 *Int. J. Mod. Phys. B* **25** 1393

[20] Liu R and Shang J X 2012 *Modelling Simul. Mater. Sci. Eng.* **20** 035020

[21] Pugh S F 1954 *Philos. Mag.* **45** 823

[22] Kresse G and Joubert D 1999 *Phys. Rev. B* **59** 1758

[23] Perdew J P, Chevary J A and Vosko S H 1992 *Phys. Rev. B* **46** 6671

[24] Monkhorst H J and Pack J D 1976 *Phys. Rev. B* **13** 5188

[25] Blanco M A, Pendas A M and Francisco E J 1996 *J. Mol. Struct. THEOCHEM.* **368** 245

[26] Birch F 1947 *Phys. Rev.* **71** 809

[27] Wang J, Neaton J B, Zheng H, Nagarajan V, Ogale S B, Liu B, Viehland D, Schlom D G, Waghmare U V, Spaldin N A, Rabe K M, Wuttig M and Ramesh R 2003 *Science* **299** 1719

[28] Neaton J B, Ederer C, Waghmare U V, Spaldin N A and Rabe K M 2005 *Phys. Rev. B* **71** 014113

[29] Hermet P, Goffinet M, Kreisel J and Ghosez P 2007 *Phys. Rev. B* **75** 220102

[30] Ricinschi D, Yun K Y and Okuyama M 2006 *J. Phys.: Condens. Matter* **18** L97

[31] Kubel F and Schmid H 1990 *Acta Crystallogr. B* **46** 698

[32] Reyes A, Vega C D L, Fuentes M E and Fuentes L J 2007 *J. Eur. Ceram. Soc.* **27** 3709

[33] Kubel F and Schmid H 1990 *Acta Crystallogr. B* **46** 698

[34] Higuchi T, Liu Y S, Yao P, Glans P A, and Guo J H 2008 *Phys. Rev. B* **78** 085106

[35] Wang H, Zheng Y, Cai M Q, Huang H T and Chan H L W 2009 *Solid State Commun.* **149** 641

[36] Hu Y F, Jiang G, Meng D Q and Kong F J 2010 *Acta Phys. Chim. Sin.* **26** 1664

[37] Lu J, Gunther A, Schrettle F, Mayr F, Krohns S, Lunkenheimer P, Pimenov A, Travkin V D, Mukhin A A and Loidl A 2010 *Eur. Phys. J. B* **75** 451

[38] Amirov A A, Batdalov A B, Kallaev S N, Omarov Z M, Verbenko I A, Razumovskaya O N, Reznichenko L A and Shilkina L A 2009 *Phys. Solid State* **51** 1189

[39] Phapale S, Mishra R and Das D 2008 *J. Nucl. Mater.* **373** 137

[40] Chen J R, Wang W L, Li J B and Rao G H 2008 *J. Alloy. Compd.* **459** 66

[41] Wang Y, Saal J E, Wu P P, Wang J J, Shang S L, Liu Z K and Chen L Q 2011 *Acta Mater.* **59** 4229

[42] Anderson O L and Zou K 1989 *Phys. Chem. Miner.* **16** 642